JOURNAL OF MAPS
2021, VOL. 17, NO. 2, 257–267
https://doi.org/10.1080/17445647.2021.1906340

SCIENCE

OPEN ACCESS Check for updates

Geology of the Macao Special Administrative Region (China)

Pedro Quelhas[a,b], Ricardo Borges[a], Ágata Alveirinho Dias[a,b], Maria Luísa Ribeiro[c], Pedro Costa[a] and João Mata[b]

[a]Institute of Science and Environment, University of Saint Joseph, Macao, People's Republic of China; [b]Instituto Dom Luiz, Faculdade de Ciências, Universidade de Lisboa, Lisboa, Portugal; [c]Laboratório Nacional de Energia e Geologia (LNEG), Lisboa, Portugal

ABSTRACT

A 1:12,000 geological map of the Macao Special Administrative Region has been produced through detailed field work supported by petrographic, mineralogical, geochronological and geochemical data obtained in previous studies. This map aims to represent a reliable tool to understand the geological evolution of the region and for management of the territory. The geology of Macao is dominated by two groups of Jurassic granitic rocks belonging to an intrusive suite located along the coast of Southeast China: Macao Group I (MGI: 164.5 ± 0.6 to 162.9 ± 0.7 Ma) and Macao Group II (MGII: 156.6 ± 0.2 to 155.5 ± 0.8 Ma), including the associated microgranite, aplite and pegmatite dikes and quartz veins. Remnants of the metasedimentary wall-rock are present as Devonian xenoliths enclosed within the granites. Younger Jurassic to Cretaceous andesite to dacite dikes (150.6 ± 0.6 to <120 Ma) intrude the granitic rocks. Additionally, Quaternary sedimentary deposits cover the older lithologies.

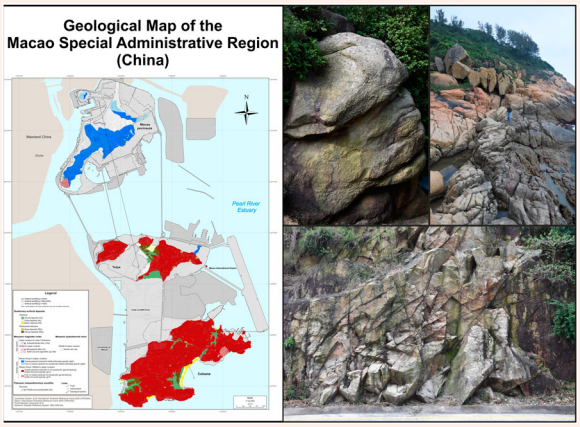

ARTICLE HISTORY
Received 16 October 2020
Revised 10 March 2021
Accepted 17 March 2021

KEYWORDS
Macao (South China); granites; geological map; magmatic rocks; Jurassic; Mesozoic

1. Introduction and previous studies

Geological maps are fundamental to understand the geological evolution of a given area, being the primary source of information for land-use planning, assessment of geological hazards and identification of ground-water aquifers and potential ore bodies. For this reason, we surveyed the Macao Special Administrative Region (SAR) and, in the light of recent petrographic, mineralogical, geochronological and geochemical data (Quelhas et al., 2020, 2021a) and previous mapping (Ribeiro et al., 1992), produced a new geological map at 1:12,000 scale.

Most of the first geological studies of Macao focused on petrography of the volumetrically dominant igneous rocks and on geological mapping (Costa, 1944; Neiva, 1944; Lemos, 1963; Carrington da Costa and Lemos, 1964). Rocha and Torquato (1967) studied the mineralogical and microfaunal composition of sands from Taipa and Coloane beaches and Marques (1988) gave a major contribution to the existing cartography and produced three 1:10,000 geological/geotechnical letters (see also Marques and Silva, 1990a, 1990b). Later, Ribeiro et al. (1992) carried out a comprehensive geological study of Macao, which includes the geological map of Macao at 1:5,000 scale and a detailed explanatory note. Additionally, this study provided the first ages of the Macao granites based on K-Ar dating of

CONTACT Pedro Quelhas pedro.quelhas@usj.edu.mo Institute of Science and Environment, University of Saint Joseph, Rua de Londres, 106, Macao SAR, China; Instituto Dom Luiz, Faculdade de Ciências, Universidade de Lisboa, Lisboa 1749–016, Portugal; Ágata Alveirinho Dias agata.dias@usj.edu.mo Institute of Science and Environment, University of Saint Joseph, Rua de Londres, 106, Macao, People's Republic of China; Instituto Dom Luiz, Faculdade de Ciências, Universidade de Lisboa, Lisboa 1749–016, Portugal

Supplemental data for this article can be accessed https://doi.org/10.1080/10376178.2018.1906340.

biotite, with most samples dated between 154 ± 5 and 168 ± 4 Ma and a younger one dated at 94 ± 2 Ma (see also Ribeiro et al., 2010).

A research project entitled '"MagIC – Petrology and Geochemistry of Igneous Rocks from Macao: Implications for the Crustal Evolution of Southern China'" (2015–2018), funded by the Macao Science and Technology Development Fund (FDCT), lead to the first two peer-reviewed publications on the geology of Macao, where high-precision zircon U-Pb geochronology of the different magmatic facies (Quelhas et al., 2020) and the petrogenesis of the granitic rocks, based on their geochemistry (Quelhas et al., 2021a), have been addressed. In sum, two chemically and age distinct groups of I-type granites have been recognized, Macao Group I (MGI: 164.5 ± 0.6 to 162.9 ± 0.7 Ma) and Macao Group II (MGII: 156.6 ± 0.2 to 155.5 ± 0.8 Ma), which, despite being derived from the same source (basaltic protolith of Paleoproterozoic–Mesoproterozoic age), had different magmatic evolution histories (Quelhas et al., 2020, 2021a). The isotope homogeneity characterizing MGII granites ($\varepsilon_{Nd}(t) \approx -8.6$ and $^{87}Sr/^{86}Sr \approx 0.7108$) has been interpreted to represent a comagmatic suite having evolved in closed system, at odds with the observed for MGI ($\varepsilon_{Nd}(t)$ ranging from–10.0 to –6.1 and initial $^{87}Sr/^{86}Sr$ between 0.7109 and 0.7201; Quelhas et al., 2021a). Evidences such as an increase in initial $^{87}Sr/^{86}Sr$ ratios with degree of evolution, presence of metasedimentary xenoliths and a relatively high percentage of zircon xenocrysts with Paleozoic ages, have shown that assimilation–fractional crystallization (AFC) processes, during which upper-crust Paleozoic metasediments were variably assimilated by MGI granitic magmas, played an important role in the evolution of MGI granites (Quelhas et al., 2021a). Moreover, magmas of the two groups underwent different fractional crystallization processes, producing distinct Rare Earth Elements (REE) evolution trends: while MGI magmas evolved by progressive enrichment in heavy REE relative to light REE mainly due to fractionation of monazite and allanite, magmas from MGII are marked by depletion of middle REE, reflecting a stronger effect of apatite and titanite fractionation (Quelhas et al., 2020, 2021a, 2021b). A mantle contribution to the genesis of Macao granitic rocks is evidenced by the occurrence of mantle-derived microgranular mafic enclaves (MME), whose abundance, mineralogy and chemical compositions also differ in the two groups (Quelhas et al., 2021a). In line with these studies, the systematics and petrogenetic model considered in the present study are those proposed by Quelhas et al. (2021a, 2021b; see also Shellnutt et al., 2020, for a different petrogenetic interpretation).

Our main aim is to integrate the findings of the above-mentioned studies with more recent field, geochronological and geochemical data to provide the first comprehensive digital version of the geological map of the Macao (at 1:12,000 scale), which will serve as an important basis for future geological studies.

2. Methods

2.1. Field work and sampling

Field studies and sampling campaigns have been carried out to produce the geologic map. Overall, 166 samples were collected during the MagIC project (see Supplementary Files 1 and 2 for details on the location and hand-sample description). Samples stored at Laboratório Nacional de Energia e Geologia (Portugal), from outcrops no longer existent due to increasing urbanization, were also studied. Detailed macroscopic analysis, complemented by petrographic/mineralogical, geochemical and geochronological data (Quelhas et al., 2020, 2021a), allowed the definition and characterization of different lithofacies.

2.2. Map construction

The digitized 1:12,000 geological map of Macao was created from the scanned cartographic base of the previous geological map surveyed at 1:5,000 scale (Ribeiro et al., 1992). The ground control points used for georeferencing were from the geodetic control points (first and second order) maintained by the government of the Macao SAR and are georeferenced to the International Terrestrial Reference Frame 2005 (ITRF2005). Vectorized layers of geological units/features were digitally drawn in the ArcGIS 10.3.1 software as ArcGIS shapefiles (polygons). Other information, such as roads and landfill limits, was sourced from the Cartography and Cadastre Bureau of Macao SAR and subsequently georeferenced. The limits of the geological units in the digitized map follow, generally, the principles set forth by the field work carried out in 1991, with improvements made after more recent field work and by using satellite imagery. An ASTER GDEM digital elevation model (DEM) Version 2 with ~30 m spatial resolution (ERSDAC, 2011) was used for generation of the digital topography, allowing to update the geological limits (sheet ASTGTM2-N22E113, acquired in 2000 and released in 2011). Additional updates to the geological units/features resulted from recent petrographic/mineralogical, geochronological and geochemical studies. The digital topography obtained from the ASTER GDEM DEM Version 2 contained some anomalies that caused inaccuracies in several areas of the map, specifically in

highly-urbanized man-made landfill areas, which prompted the need to manually review all individual pixels of the satellite imagery pertaining to these areas and correct them accordingly. Concerning the limits of landfills, the new geological map shows with more detail the evolution of man-made landfill expansion from the time of the previous geological map to the present day. Dates are shown in order to aid interpretation, with a scheme design following the method applied by the Survey and Mapping Office (SMO) of the Hong Kong Special Administrative Region on their 1:20,000 (Series: HGM20) geological maps (SMO, 2020). Archival sources, like maps, urban plans and aerial photography, provided dating information of the landfill evolution, which is represented on the map in three shades of gray, contrasting the landfill construction from the nineteenth, twentieth and twenty-first centuries, as well as with number labels corresponding to the construction year of different landfills.

3. Geology

3.1. Geological background

Macao is located in southern Guangdong province, along the coast of SE China, on the western margin of the Pearl River Delta (PRD; see inset map and Figure 1). In this region, there is an abudance of granitic intrusions belonging to the NE-trending Mesozoic Southeast China Magmatic Belt, outcropping in the southeastern part of the Cathaysia Block (see inset map). The stratigraphic sequence consists of a metasedimentary Neo-proterozoic basement overlain by a discontinuous Paleozoic to Mesozoic terrigenous sequence with carbonate units, which is intruded by widespread Jurassic to Cretaceous granitic and volcanic rocks (Figure 1).

Three main structural domains are identified according to their dominant direction (NE-SW, NW-SE and W-E; Figure 1). The NE-SW system is the most prominent, whereas the other two mostly intersect the NE-SW system and have a lesser expression (e.g. Lancia et al., 2020). The emplacement of granitic bodies was controlled by large-scale regional NE-trending fault zones (Figure 1; Ribeiro et al., 1992; Xia and Zhao, 2014). Some of these regional structures constrained magma ascent during regional plutonism and volcanism (Figure 1; Xia and Zhao, 2014) and shaped the morphology of the PRD basin and coast line (Lancia et al., 2020). One of the most important tectonic structures in the coastal region of SE China is the NE-trending Zhenghe-Dapu Fault (ZDF) zone, which can be traced for over 400 km through the coastal provinces of SE China (see inset map and Figure 2) and is thought to separate the western and eastern Cathaysia blocks (e.g. Xu et al., 2007). Near Macao and Hong Kong, the ZDF comprises a ~30 km wide zone limited to the north and to the south by the Shenzhen and the Haifeng faults, respectively (Figure 1) and is associated with several Late Mesozoic volcanic centers and plutonic assemblages (e.g. Sewell and Campbell, 1997; Xia and Zhao, 2014). Geochronological data has shown that the granitic rocks intruded as discrete magmatic pulses separated by periods of a few million years of magmatic quiescence, suggesting that granitic plutons were incrementally assembled (Quelhas et al, 2020; Sewell et al., 2012).

To the west and north of Macao, most of the granitoids intruded Paleozoic strata, as large plutons and/or batholiths, during the Jurassic period (165–150 Ma; e.g. Quelhas et al., 2020; Huang et al., 2013). On the eastern margin of the PRD, Mesozoic volcanic-plutonic rocks of Jurassic to Early Cretaceous age (165–140 Ma; Sewell et al., 2012) intruded Late Paleozoic and Early to Middle Jurassic sedimentary successions (Figure 1).

Although the PRD region corresponds to a Neo-Paleozoic depression, superimposed and reworked by several Paleozoic to Mesozoic tectonic events, the Pearl River drainage basin was formed during the Cenozoic due to uplift of the Tibetan Plateau (Zong et al., 2009; Lancia et al., 2020) and has been influenced by several transgression events since the early Pleistocene (Zong, 2004). Until the Late Quaternary, sediments from the drainage system bypassed the receiving basin and were deposited on the continental shelf and slope of the northern South China Sea (Zong et al., 2009). During the Late Quaternary, however, active fault systems caused land subsidence of the receiving basin, leading to the deposition of terrestrial and marine sedimentary units that overly Cretaceous–Paleogene sandstones and Mesozoic granites (Zong et al., 2009 and references therein).

The geology of Macao is dominated by granitic intrusions, belonging to a batholith extending about 50 km to the north (Figure 1). These intrusions form hills that stand out from adjacent landscape due to their high relief (see geological sections accompanying the map). Among the magmatic rocks, biotite granites, with variable textural and mineralogical characteristics, predominate. They contain MME and metasedimentary xenoliths and are intruded by a relatively diversified swarm of granitic and andesitic/dacitic dikes and quartz veins. Below, a detailed description of each lithofacies is provided.

3.2. Lithofacies

3.2.1. Magmatic rocks

3.2.1.1. Granitic rocks. Most of Macao granitic intrusions are covered by dense vegetation, leaving scarce

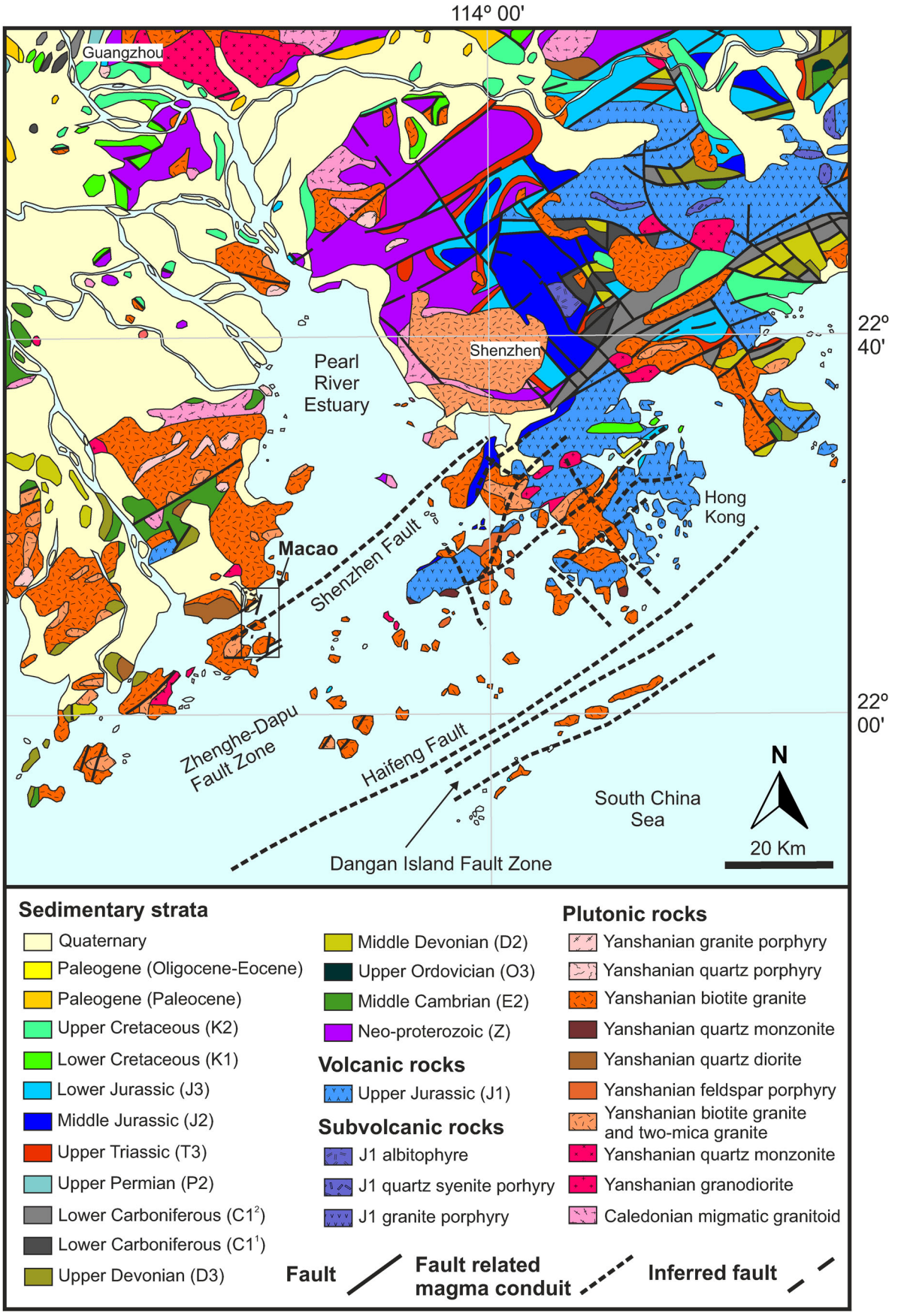

Figure 1. Geological map of the Pearl River Delta region (adapted from Guangdong, 1988; Xia and Zhao, 2014). Yanshanian magmatic rocks were formed during the Jurassic–Cretaceous period.

and weathered outcrops of meter-wide rounded boulders, either isolated or in chaotic jumbles of large boulders (Figure 2a). This, together with the increasing urbanization of the territory, has made difficult the observation of field relationships between different granitic facies. The best exposures are those

Figure 2. Representative outcrops of granitic rocks of Macao. (a) Rounded granitic boulder on a hill in Taipa; (b) Deformed granites along a shear zone in a coastal area of Coloane; (c) Granitic rocks exposed in a road cut in Taipa, showing joints formed due to thermal stress during the cooling of the pluton.

of massive granites found along the coastline (Figure 2b) and road cuts (Figure 2c).

Two groups of biotite granites have been recognized in Macao: microcline-bearing (MGI: 164.5 ± 0.6 to 162.9 ± 0.7 Ma; Figure 3a–d) and orthoclase-bearing (MGII: 156.6 ± 0.2 to 155.5 ± 0.8 Ma; Figure 3e and f) granites (Quelhas et al., 2020). The different K-feldspar structures have been identified in hand specimen by the gray whitish color of microcline as opposed to the pinkish color of orthoclase and also, under microscope, by different types of twinning (albite/pericline vs. Carlsbad, respectively; Quelhas et al., 2020). Although most of the mineralogical components are common, there are differences in the occurrence and abundance of specific accessory phases, mineral chemistry and whole-rock chemistry among the two groups.

In both groups, the porphyritic coarse-grained granitic facies often host MME, easily recognized in the field by their dark color (Figure 3d and f). Compared with the host granite, MME generally contain a similar mineral assemblage, but with higher contents of biotite and plagioclase, and lower contents of quartz and alkali feldspar (Quelhas et al., 2021a).

MGI granites are significantly more deformed than MGII granites as evidenced by several microscopic features such as strong undulatory

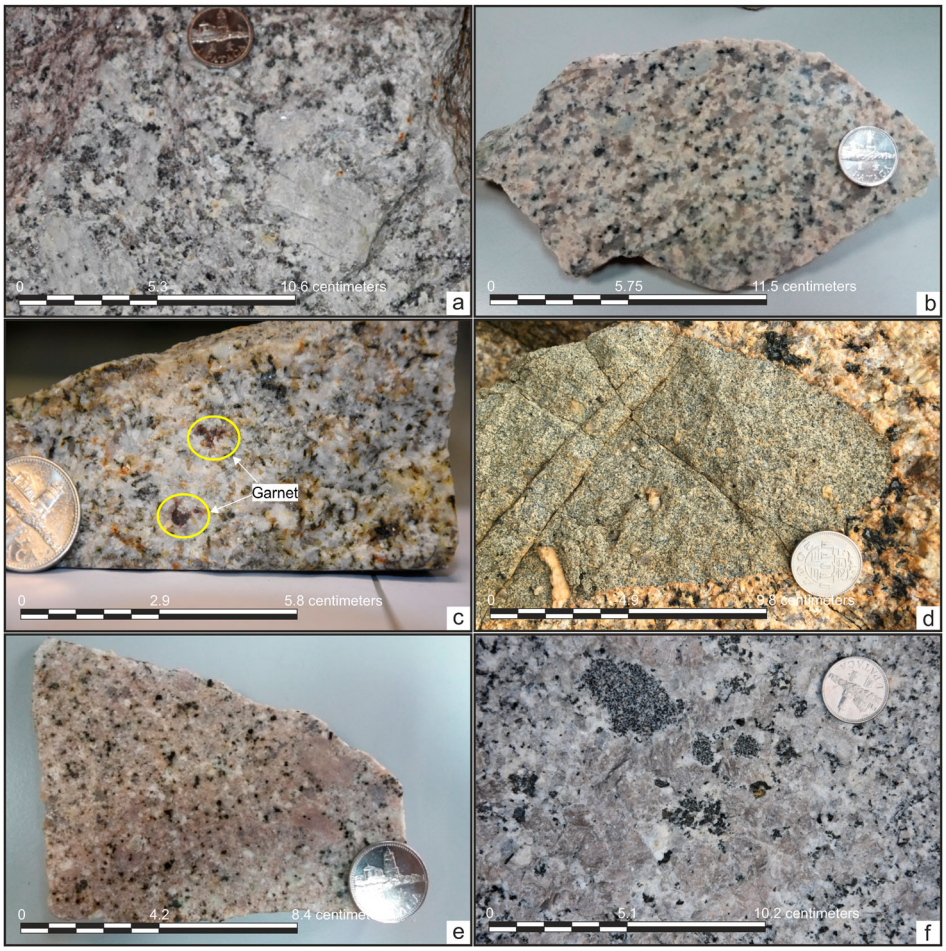

Figure 3. Granitic facies of Macao. (a) MGI very coarse-grained porphyritic biotite-microcline granite from Coloane; (b) MGI coarse-grained non-porphyritic garnet-bearing biotite-microcline granite from Taipa; (c) MGI fine- to medium-grained non-porphyritic garnet-bearing granite from Coloane, with large brownish red garnet grains; (d) MGI MME from Coloane, showing a K-feldspar crossing the boundary between the MME and the host granite; (e) MGII coarse-grained porphyritic biotite-orthoclase granite from Macao Peninsula; (f) MGII MME from Macao Peninsula surrounded by pinkish orthoclase megacrysts. MME – microgranular mafic enclaves.

extinction, subgranulation and bands of crushed minerals (e.g. quartz and alkali feldspar; see Quelhas et al., 2020). The ubiquitous presence of microcline in this group has also been interpreted as being suggestive of high degrees of deformation, which may have acted as an external mechanism for the inversion of an earlier monoclinic (orthoclase) to a triclinic (microcline) K-feldspar phase (Quelhas et al., 2020).

3.2.1.1.1. Macao Group I (MGI). The MGI granites outcrop in Taipa and Coloane areas, though a small occurrence in the southernmost tip of Macao Peninsula has been also identified. Overall, they are gray to whitish in color and have as major mineral components quartz (30–35 vol%), alkali feldspar (35–40 vol%) and plagioclase (20–25 vol%), with minor amounts of biotite (10–15 vol%; these percentages are approximate estimates based on detailed petrographic observation of several thin sections). This group can be further divided into two sub-groups based on grain size and mineralogy (see map; Figure 3a and b).

The porphyritic varieties, characterized by the presence of large microcline megacrysts, vary from very coarse-grained in Coloane (Figure 3a) to medium- to coarse-grained in Taipa. Compared to porphyritic varieties, the non-porphyritic ones are characterized by comparatively smaller grain size, xenomorphic texture and by the occurrence of garnet as accessory phase (Figure 3b). In addition, small stocks of fine- to medium-grained non-porphyritic garnet-bearing biotite-microcline granites occur in Macao Peninsula and Coloane and have as distinctive mineralogical features the occurrence of large garnet grains and acicular biotite (Figure 3c).

Metasedimentary xenoliths are frequently hosted by the non-porphyritic facies (Figure 5c). MGI MME (Figure 3d) have variable sizes (centimeter to decimeter-wide, up to 1 meter in width) and vary from monzogranite to granodiorite, containing acicular biotite and no accessory titanite. They occur as irregular blobs, oval and elongated in shape, with sharp contacts with the host granite (Figure 3d). Textures vary from slightly porphyritic with alkali feldspar

megacrysts to fine-grained equigranular hypidiomorphic (Quelhas et al., 2021a).

3.2.1.1.2. Macao Group II (MGII). The less abundant MGII granites mainly outcrop in Macao Peninsula, with a small outcrop in the easternmost tip of Taipa. They are pinkish in color (Figure 3e and f) and their major mineralogical components are quartz (30–35 vol%), alkali feldspar (35–40 vol%), plagioclase (20–25 vol%) and biotite (10–15 vol%). No garnet has been identified in this group and, contrasting with MGI granites, euhedral titanite is particularly abundant and well-developed (Quelhas et al., 2020). According to textural and mineralogical features, this group can be further divided into two sub-groups: (1) coarse-grained porphyritic biotite-orthoclase granite (Figure 3e) and; (2) fine- to medium-grained non porphyritic biotite-orthoclase granite.

No metasedimentary xenoliths have been found in this group. Quelhas et al. (2021a) has interpreted this observation based on the fact that the MGI granites (at least ~6 Ma older than MGII) intruded the upper crust, facilitating the assimilation of supracrustal sedimentary materials, whereas the second granitic pulse (MGII) took the ascension route previously followed by MGI magmas, intruding the MGI granites at shallow crustal levels. Therefore, MGI granites acted as the wall rock for MGII granitic magmas rather than the supracrustal sedimentary strata, precluding the possibility of significant assimilation of sedimentary materials in MGII (Quelhas et al., 2021a).

MGII MME are distinguished from MGI MME by their comparatively smaller size (Figure 3f). They are mostly quartz monzodiorites and contain abundant titanite and, in some cases, hornblende. They have sharp to diffusive contacts with their host and occur as centimeter to decimeter-wide round-shaped blobs. The texture varies from fine- to medium-grained slightly porphyritic (with orthoclase megacrysts) to fine-grained moderately equigranular hypidiomorphic (Quelhas et al., 2021a).

3.2.1.2. Felsic dikes

3.2.1.2.1. Microgranite dikes. Microgranite dikes (Figure 4a and b) tendo to be more abundant in some areas of the territory (e.g. northeastern areas of Taipa main intrusions) and display a wide range of

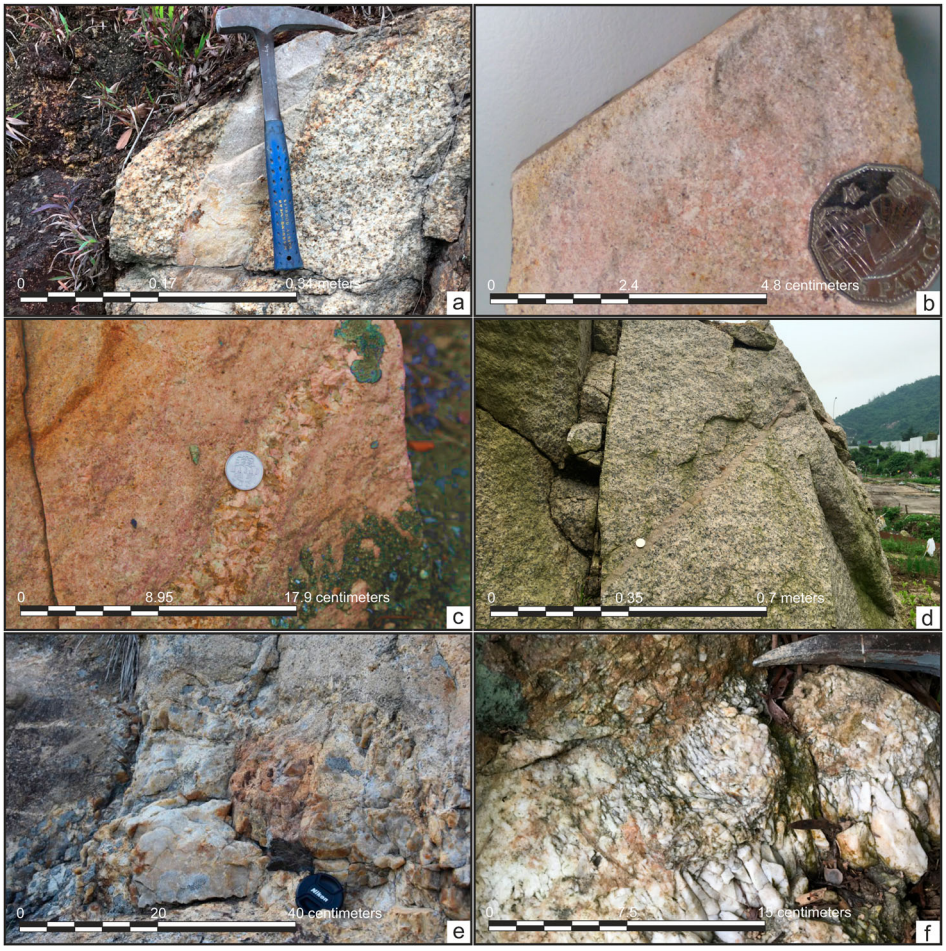

Figure 4. Granitic dikes of Macao. (a) Microgranite dike cutting the MGI coarse-grained porphyritic biotite-microcline granite from Taipa; (b) Fine-grained equigranular texture of a microgranite dike; (c) Aplite-pegmatite dike with the pegmatite in the center bordered by aplite; (d) Aplite vein cutting the MGI coarse-grained porphyritic biotite-microcline granite from Coloane; (e) Pod-shaped pegmatite associated with the MGI fine- to medium-grained non-porphyritic garnet-bearing biotite-microcline granite from Coloane; (f) Quartz vein with centimeter-long crystals growing perpendicularly to the vein wall.

widths (from centimeter to meter-wide). They are leucocratic (in some cases slightly pinkish due to K-feldspar alteration) and have a fine-grained (<0.1 cm) moderately equigranular xenomorphic texture (Figure 4b).

3.2.1.2.2. Aplite/pegmatite dikes. Aplites and pegmatites show diffuse irregular (Figure 4c) to relatively sharp (Figure 4d) contacts against the host granite. Pegmatites occur essentially as dikes cross-cutting fine-grained granitic facies or, more rarely, as pod-shaped bodies within the granites (up to 1 meter in width; see Figure 4e). Aplite dikes are centimeter- to decimeter-wide and are characterized by a very fine-grained (<0.1 cm) moderately equigranular xenomorphic texture with abundant garnet crystals as accessory mineral (Quelhas et al., 2021a). These two lithotypes have been mapped with the same symbol (although with distinct labels indicating the predominant lithotype in a given dike) due to the fact that they represent magmatic liquids of similar degree of evolution and often occur together as composite dikes with gradual variations between pegmatitic and aplitic textures (Figure 4c).

3.2.1.3. Quartz veins. Quartz veins are abundant and intrude all the above-mentioned granitic rocks and dikes. They are usually centimeter to decimeter-wide, with some reaching larger sizes (> 0.5 m), and the contact with the host granites is sharp and regular. Quartz is usually massive and milky, though hyaline euhedral prismatic crystals with lengths of some centimeters (<10 cm), growing parallel to each other and perpendicularly to the fracture, have also been identified in the larger veins (Figure 4f).

3.2.1.4. Andesite/dacite dikes. Despite being relatively rare, andesite/dacite dikes (150.6 ± 0.6 to <120 Ma; Quelhas et al., 2020) are found cutting all the granitic facies (Figure 5a). In Taipa, these dikes have variable widths (decimeter to meter-wide) with sharp contacts against the host granite, while in Coloane they often occur as small enclaves or lenticular bodies with well-defined regular contours. Their texture varies from aphanitic to slightly porphyritic with euhedral to subhedral tabular plagioclase (<0.5 cm) and prismatic amphibole (<0.1 cm) phenocrysts within an aphanitic matrix mainly composed of K-feldspar and microcrystalline quartz and minor Fe-Ti oxides (Quelhas et al., 2020). In the field, they are recognized by a greenish color (Figure 5b) due to the presence of chlorite and epidote, which formed by variable degrees (moderate to strong) of post-magmatic alteration.

3.2.2. Metasedimentary rocks

The metasedimentary rocks consist of altered fine-grained quartz-rich pelites of Devonian age (as estimated through lithologic correlation with similar units in neighboring areas; Ribeiro et al., 1992), which outcrop in Coloane as meter-wide (<1,5 m) xenoliths enclosed within the granites (Figure 5c). These xenoliths show slaty cleavage with variable direction and, in some cases, being discordant with

Figure 5. Other magmatic and metamorphic lithofacies of Macao. (a) Dacite dike intruding highly altered MGI granitic rocks in Taipa; (b) Dacite dike with some quartz amygdales within an aphanitic texture; (c) Metasedimentary xenolith hosted and intruded by the MGI fine- to medium-grained non-porphyritic biotite-microcline granite in Coloane.

the direction of the sharp contacts against the host granite, indicating that they have been foliated prior to the emplacement of the granites. They are mainly composed of variable proportions of quartz, plagioclase, white mica, titanite and Ti-Fe oxides.

3.2.3. Surficial sedimentary deposits

The youngest lithologies in Macao consist of Holocene–Pleistocene sedimentary deposits of marine, river and continental nature. Most of these sediments originated from weathering processes in subtropical conditions and were accumulated in basins created by fracturing/faulting of the granitic rocks since the Late Mesozoic (Marques, 1988; Ribeiro et al., 1992). Five types of deposits can be recognized (see also Ribeiro et al., 1992 and references therein): (1) arkose deposits: fluvial quartz- and feldspar-rich sandstones with kaolinitic matrix (Figure 6a), occasionally intercalated with decimeter-wide lenses of clay-rich sediments and ferruginous sandstone; (2) slope deposits: alluvial conglomerates composed of coarse-grained heterogranular clasts of granitic rocks, quartz and other lithologies, agglutinated by a clay-sandy matrix of brownish red color; (3) beach deposits: sands of fluvial-marine origin containing a wide range of mineralogical components, mostly derived from local lithologies, where the high percentage of chlorite, biotite, clay and oxides often confers them a dark color (Figure 6b); (4) coast deposits: fine-grained poorly polished sands showing evidence for aeolian transport; (5) alluvial deposits (Figure 6c): fine-grained brown to black color clay-rich sediments, with high percentage of organic matter and some percentage of sand-silt component.

Figure 6. Surficial sedimentary deposits of Macao. (a) Arkose deposit in Coloane; (b) Beach sediments in Coloane; (c) Alluvial sediments in Taipa.

In addition to these, Holocene fluvial-marine and Pleistocene alluvial units have also been recognized offshore from borehole stratigraphies (see geological sections accompanying the main map and also Marques, 1988; Ribeiro et al., 1992). The geological sections show that the thickness of the Quaternary deposits is variable and controlled by the morphology of the underlying granitic bedrock, though a maximum thickness of around 25 meters is estimated for the Holocene sequence (geological section C–D). The coast, beach and alluvial deposits outcropping in the territory are proximal facies of the Holocene sedimentary sequence, having as more distal facies fluvial-marine deposits characterized by different proportions of sand, silt and clay components (see geological sections C–D and E–F). The Pleistocene–Holocene arkose and slope deposits, on the other hand, are more proximal equivalents of the Pleistocene alluvial deposits identified by Marques (1988).

3.3. A brief note on the structural geology

An extensive and detailed study of the structural geology of Macao has been conducted by Ribeiro et al. (1992). In the current version of the geological map of Macao SAR no changes to this aspect are proposed and only confirmed faults in the field were represented (except for the inferred geological limit between MGI and MGII granites in Taipa). Overall, two main structural systems (ENE-WSW and NW-SE) and four secondary ones (NE-SW; N-S to NNE-SSW; W-E; and NW-SE) have been recognized in Macao (see Ribeiro et al., 1992 for more details).

Ribeiro et al. (1992) has assigned some of the fracture and fault systems affecting the granites to one cycle of deformation related to the Yanshanian Orogeny; however, the authors also emphasize a possible subsequent influence of the, still active, Shenzhen-Wuhua fault zone (Figure 1), which is concordant with one of the main fracture systems (ENE-WSW)

in Macao (also continuous throughout the PRD region; e.g. Sun et al., 2010). Although the opening of the NE-trending PRD basin is thought to have occurred during the Early Cenozoic (e.g. Zhou et al., 1995), previous studies suggest that the formation of the PRD basin was strongly controlled by pre-Cenozoic structures (e.g. Sun et al., 2010). In Macao, this precept is reinforced by the resetting of the K-Ar system in biotites of Jurassic granites during the Late Cretaceous (94 ± 2 Ma) near an important ENE-WSW-trending shear zone in Coloane (Quelhas et al., 2020), suggesting pre-Cenozoic tectonic activity in the territory.

4. Conclusions

The new geological map of Macao represents an accurate and updated basis for understanding the geological evolution of this area of SE China. The map has relevance for the understanding of the Late Mesozoic magmatic evolution in the region, as it provides new insights into the distribution of magmatic rocks, at large scale (1:12,000), in this area of the PRD. The map includes an updated stratigraphic reconstruction of the Macao intrusive suite lithologies and their age. It also represents an invaluable contribution towards the knowledge of the geological diversity of the territory, which may have important implications not only for future geological studies but also to other relevant areas such as engineering, urban planning and environmental sciences.

Software

Georeferencing and digitization were performed using ESRI ArcGis 10.3.1. Correction of anomalies in the digital topography was performed with QGIS 2.18.3. The final map layout and pictures were produced using CorelDRAW X8.

Acknowledgements

This research was supported by the Macao Science and Technology Development Fund (FDCT 043/2014/A1). We acknowledge the financial FCT support through project UIDB/50019/2020 – IDL. We also thank LNEG (Portugal) and LECM (Macau) for providing samples from sites that are no longer available due to the extensive construction and Lou U. Tat for his help during field and lab work.

Disclosure statement

No potential conflict of interest was reported by the authors.

Funding

This work was supported by Fundo para o Desenvolvimento das Ciências e da Tecnologia [grant number FDCT 043/2014/A1]; Fundação para a Ciência e a Tecnologia [grant number UIDB/50019/2020 – IDL].

Data availability statement

The authors confirm that the data supporting the findings of this study are available within the article and its supplementary materials.

References

Carrington da Costa, J., & Lemos, M. S. (1964). Fisiografia e Geologia da Província de Macau: Centro de Informação e Turismo, 53 p.

Costa, J. C. D. A. (1944). Geologia da Província de Macau. *Boletim da Sociedade Geológica de Portugal*, *3*, 181–222.

Earth Remote Sensing Data Analysis Center (ERSDAC). (2011). ASTER GDEM. https://asterweb.jpl.nasa.gov/gdem.asp

Huang, H.-Q., Li, X.-H., Li, Z.-X., & Li, W.-X. (2013). Intraplate crustal remelting as the genesis of Jurassic high-K granites in the coastal region of the Guangdong Province, SE China. *Journal of Asian Earth Sciences*, *74*, 280–302. https://doi.org/10.1016/j.jseaes.2012.09.009

Lancia, M., Su, H., Tian, Y., Xu, J., Andrews, C., Lerner, D. N., & Zheng, C. (2020). Hydrogeology of the Pearl River Delta, southern China. *Journal of Maps*, *16*(2), 388–395. https://doi.org/10.1080/17445647.2020.1761903

Lemos, M. S. (1963). *Esboço Geológico da Província Ultramarina de Macau, Escala 1/25000*. Centro de Informação e Turismo.

Marques, F. M. S. F. (1988). *Contribuição para o conhecimento geológico e geotécnico do Território de Macau*. Faculdade de Ciências da Universidade de Lisboa, 184 p.

Marques, F. M. S. F., & Silva, M. O. (1990a). Geotechnical properties and provenance of the Pleistocene alluvium of Macau. In A. A. (Ed.), *VIth international congress international association of engineering geology* (pp. 2899–2905). Balkema.

Marques, F. M. S. F., & Silva, M. O. (1990b). Geotechnical properties of the Holocene muds of Macau. *Geolis*, *4*, 177–191.

Neiva, J. M. C. (1944). Rochas eruptivas da Península de Macau e das ilhas de Taipa e Coloane. *Boletim da Sociedade Geológica de Portugal*, *3*, 145–180.

Quelhas, P., Dias, Á. A., Mata, J., Davis, D. W., & Ribeiro, M. L. (2020). High-precision geochronology of Mesozoic magmatism in Macao, Southeast China: Evidence for multistage granite emplacement. *Geoscience Frontiers*, *11*(1), 243–263. https://doi.org/10.1016/j.gsf.2019.04.011

Quelhas, P., Mata, J., & Dias, Á. A. (2021a). Evidence for mixed contribution of mantle and lower and upper crust to the genesis of Jurassic I-type granites from Macao, SE China. *GSA Bulletin*, *133*(1-2), 37–56. https://doi.org/10.1130/B35552.1

Quelhas, P., Mata, J., & Dias, Á. A. (2021b). Magmatic evolution of garnet-bearing highly fractionated granitic rocks from Macao, Southeast China: Implications for granite-related mineralization processes. *Journal of Earth Science,* in press. https://doi.org/10.1007/s12583-020-1389-4

Ribeiro, M. L., Ramos, J. F., Pereira, E., & Dias, R. (2010). The evolution of the Macao geological knowledge. *Geologia das Ex-Colónias da Ásia e Oceânia, Macau*, *III*, 259–266.

Ribeiro, M. L., Ramos, J. M., Pereira, E., & Dias, R. P. (1992). *Notícia Explicativa da Carta Geológica de Macau na escala 1/5000*. Serviços Geológicos de Portugal, 46 p.

Rocha, A. T., & Torquato, J. R. (1967). Contribuição para o conhecimento da mineralogia das areias de praia das Ilhas da Taipa e de Coloane (Província Portuguesa de Macau). *Bol. Inst. Invest. Cient. de Angola*, *4*, 89–104.

Sewell, R. J., & Campbell, S. D. G. (1997). Geochemistry of coeval Mesozoic plutonic and volcanic suites in Hong Kong. *Journal of the Geological Society*, *154*(6), 1053–1066. https://doi.org/10.1144/gsjgs.154.6.1053

Sewell, R. J., Davis, D. W., & Campbell, S. D. G. (2012). High precision U–Pb zircon ages for Mesozoic igneous rocks from Hong Kong. *Journal of Asian Earth Sciences*, *43*(1), 164–175. https://doi.org/10.1016/j.jseaes.2011.09.007

Shellnutt, J. G., Vaughan, M. W., Lee, H. Y., & Iizuka, Y. (2020). Late Jurassic Leucogranites of Macau (SE China): A record of crustal recycling during the early Yanshanian Orogeny. *Frontiers in Earth Science*, *8*, 1–24. https://doi.org/10.3389/feart.2020.00001

Sun, Z., Zhou, D., Sun, L., Chen, C., Pang, X., Jiang, J., & Fan, H. (2010). Dynamic analysis on rifting stage of Pearl River Mouth basin through analogue modeling. *Journal of Earth Science*, *21*(4), 439–454. https://doi.org/10.1007/s12583-010-0106-0

Survey and Mapping Office. (2020). *Lands Department, Hong Kong Special Administrative Region*. https://www.landsd.gov.hk/mapping/en/paper_map/gm.htm

Xia, S., & Zhao, D. (2014). Late Mesozoic magmatic plumbing system in the onshore-offshore area of Hong Kong: Insight from 3-D active-source seismic tomography. *Journal of Asian Earth Sciences*, *96*, 46–58. https://doi.org/10.1016/j.jseaes.2014.08.038

Xu, X., O'Reilly, S. Y., Griffin, W. L., Wang, X., Pearson, N. J., & He, Z. (2007). The crust of Cathaysia: Age, assembly and reworking of two terranes. *Precambrian Research*, *158*(1-2), 51–78. https://doi.org/10.1016/j.precamres.2007.04.010

Zhou, D., Ru, K., & Chen, H.-Z. (1995). Kinematics of Cenozoic extension on the South China Sea continental margin and its implications for the tectonic evolution of the region. *Tectonophysics*, *251*(1-4), 161–177. https://doi.org/10.1016/0040-1951(95)00018-6

Zong, Y. (2004). Mid-Holocene sea-level highstand along the Southeast coast of China. *Quaternary International*, *117*(1), 55–67. https://doi.org/10.1016/S1040-6182(03)00116-2

Zong, Y., Yim, W. W. S., Yu, F., & Huang, G. (2009). Late Quaternary environmental changes in the Pearl River mouth region, China. *Quaternary International*, *206*(1-2), 35–45. https://doi.org/10.1016/j.quaint.2008.10.012